An effective solution of electro-thermo-structural problem of uni-axially graded material

J. Murín[†], V. Kutiš[‡] and M. Masný[‡†]

Slovak University of Technology, Faculty of Electrical Engineering and Information Technology Department of Mechanics, Bratislava 812 19 Slovak Republic

Abstract. The aim of this contribution is to present a new link/beam finite element suitable for electro-thermo-structural analysis of uni-axially graded materials. Continuous polynomial variation of geometry and material properties will be considered. The element matrix and relations for solution of Joule's heat (and its distribution to the element nodes) have been established in the sense of a sequence method of a coupled problem solution. The expression for the solution of nodal forces caused by a continuously distributed temperature field has also been derived. The theoretical part of this contribution is completed by numerical validation, which proves the high accuracy and effectiveness of the proposed element. The results of the performed experiments are compared with those obtained using the more expensive multiphysical link element and solid element of the FEM program Ansys. The proposed finite element could be used not only in the multiphysical analysis of the current paths and actuators but also in analysis of other 1D construction parts made of composite or uni-axially graded materials.

Keywords: FEM; uni-axially graded materials; coupled problems.

1. Introduction

Materials that are made by mixing two or more different materials together (evenly or unevenly) can acquire much better properties than their single components. These new materials (composite or functionally graded-FGM (http://www.eumat.org 2006, Koizumi 1997, Koizumi and Niino 1995, FGM Forum 1991, Müller *et al.* 2003, Kawasaki and Watanabe 1997) are characterized with a continuous or discontinuous variation of material properties. Simultaneously with the production of such materials, new numerical methods have been developed and the existing methods have been enhanced for their numerical simulation.

The most frequent area of application of such new materials is mechatronics, where a solution of multiphysical problems has to be found (weak or strong coupled) (Felippa and Park 2004). For example, in an electro-thermo-structural problem the electric losses cause the accompanying or required deformation of the actuator (or of the conductor path) by the generated Joule's heat. Comercial FEM programs contain link and solid elements with constant or average material

---

† Professor Ing., Corresponding author, DrSc., E-mail: justin.murin@stuba.sk
‡ Ing., Ph.D., E-mail: vladimir.kutis@stuba.sk
‡† Ing., Ph.D., E-mail: michal.masny@stuba.sk

properties, e.g. (ANSYS 2007). These elements can also be used for analysis of functionally graded materials but the solution accuracy very strongly depends on the mesh density and preparation of input data is very time consuming. This disadvantage could be particularly removed by using meshless methods (Atluri and Shen 2004) or by improving classical finite elements (Chakraborty *et al.* 2003, Zhu and Sankar 2004, Lee 2005, Agarwal *et al.* 2006).

The aim of this contribution is to establish expressions of a new beam finite element for solution of weak coupled electro-thermo-structural problem with a sequence method. This element can have a longitudinally varying cross-section (cross-sectional area and area moment of inertia) and uni-axially graded material properties (electrical and thermal conductivity, elasticity modulus and thermal expansion coefficient). The element matrix contains transfer constants which depend on the material properties and the cross-sectional variation. A simple numerical algorithm for solution of these transfer constants will be proposed as well.

All the main equations of this new element will be satisfied exactly and the solution accuracy will not depend on the mesh density. The accuracy and effectiveness of the derived beam element will be shown by the solution of chosen multiphysical problems.

2. Definition of the geometry and material properties variation

Fig. 1 shows a 2D beam element with variation of geometry (cross-sectional area $A(x)$ and area moment of inertia $I_y(x)$) and material properties (electrical conductivity $\sigma(x)$, thermal conductivity $\lambda(x)$, thermal expansion coefficient $\alpha_T(x)$ and elasticity modulus $E(x)$) along the element length L. We assume that all previously mentioned geometry and material parameters can be expressed in polynomial form − see the following sections.

2.1 Variation of geometry

2.1.1 Variation of cross-sectional area
Variation of the cross-sectional area is defined by the polynomial

$$A(x) = A_i \eta_A(x) = A_i \left(1 + \sum_{k=1}^{n} \eta_{Ak} x^k \right)$$

(1)

where A_i is the cross-sectional area at node i and polynomial $\eta_A(x)$ expresses the variation of the cross-sectional area along the element length L. The order of this polynomial is n. Constants η_{Ak}, where $k = 1, ..., n$, and the order n of the polynomial depend on the cross-sectional area variation.

2.1.2 Variation of area moment of inertia
Variation of the area moment of inertia is defined in a similar way

$$I_y(x) = I_{yi} \eta_I(x) = I_{yi} \left(1 + \sum_{k=1}^{p} \eta_{Ik} x^k \right)$$

(2)

where I_{yi} is the area moment of inertia at node i and polynomial $\eta_I(x)$ expresses the variation of the area moment of inertia along the element length L. Constants η_{Ik} and order p have a similar meaning as in the cross-sectional area variation mentioned above.
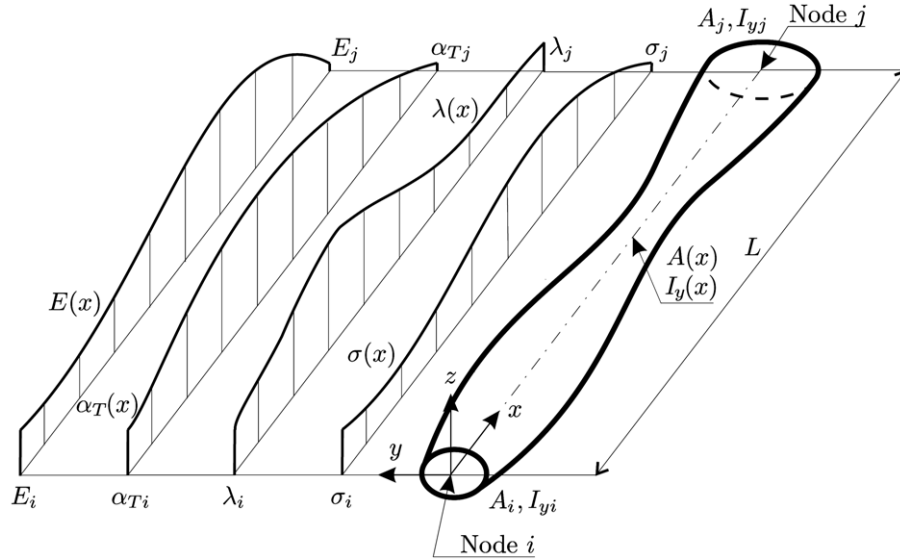
Fig. 1 Beam element with variation of geometry and material properties

2.2 Variation of material properties

2.2.1 Electrical conductivity variation

Electrical conductivity is a material property which depends on the type of material and temperature. For example, if the beam in Fig. 1 is produced by a powder metallurgy process with a non-uniform composition of powders along the element length, the material properties will vary along the element length. The continuously varying electrical conductivity of the link conductor is assumed in the polynomial form

$$\sigma(x) = \sigma_i \eta_\sigma(x) = \sigma_i \left(1 + \sum_{k=1}^{q} \eta_{\sigma k} x^k \right) \tag{3}$$

where σ_i is the electrical conductivity at node i, and $\eta_\sigma(x)$ is the polynomial of varying conductivity along the element length L - see Fig. 1. Its constants $\eta_{\sigma k}$, where $k = 1, ..., q$, and the order q of the polynomial depend on the conductivity variation.

2.2.2 Thermal conductivity variation

Thermal conductivity as well as electrical conductivity are material properties which depend on the type of material and temperature.

The variation of thermal conductivity will be assumed in polynomial form as

$$\lambda(x) = \lambda_i \eta_\lambda(x) = \lambda_i \left(1 + \sum_{k=1}^{r} \eta_{\lambda k} x^k \right) \tag{4}$$

where λ_i is the value of thermal conductivity at node i and $\eta_\lambda(x)$ expresses the variation along the element length L - see Fig. 1. Constants $\eta_{\lambda k}$ and the order r have a similar meaning as in the electrical conductivity variation mentioned above.

2.2.3 Thermal expansion coefficient variation

Variation of the thermal expansion coefficient will be assumed in a similar polynomial form

$$\alpha_T(x) = \alpha_{Ti}\eta_\alpha(x) = \alpha_{Ti}\left(1 + \sum_{k=1}^{s}\eta_{\alpha k}x^k\right) \tag{5}$$

where α_{Ti} is the value of thermal conductivity at node i, and $\eta_\alpha(x)$ expresses its variation. Constants $\eta_{\alpha k}$ and the order of polynomial s depend on the thermal expansion coefficient variation.

2.2.4 Elasticity modulus variation

Variation of the elasticity modulus will be assumed in a similar polynomial form as above

$$E(x) = E_i\eta_E(x) = E_i\left(1 + \sum_{k=1}^{t}\eta_{Ek}x^k\right) \tag{6}$$

where E_i is the value of thermal conductivity at node i, and $\eta_E(x)$ expresses its variation. Its constants η_{Ek} and the order of polynomial t depend on elasticity modulus variation.

3. FEM equations for the weak coupled electro-thermo-structural problem

The basic FEM equations of the multiphysical link/beam finite element according to the sequence solution method of the weak coupled electro-thermo-structural problem have the form

$$\begin{bmatrix} \mathbf{K}_V^e & \mathbf{0} & \mathbf{0} \\ \mathbf{0} & \mathbf{K}_T^e & \mathbf{0} \\ \mathbf{0} & \mathbf{0} & \mathbf{K}_u^e \end{bmatrix}\begin{bmatrix} \mathbf{V}^e \\ \mathbf{T}^e \\ \mathbf{u}^e \end{bmatrix} = \begin{bmatrix} \mathbf{I}^e \\ \mathbf{P}^e(\mathbf{V}) \\ \mathbf{F}^e(\mathbf{T}) \end{bmatrix} \tag{7}$$

where $\mathbf{K}_V^e$ is the electric conductance matrix, $\mathbf{K}_T^e$ is the thermal conductance matrix, $\mathbf{K}_u^e$ is the stiffness matrix, $\mathbf{V}^e$ is the vector of nodal electric potentials, $\mathbf{T}^e$ is the vector of nodal temperatures, $\mathbf{u}^e$ is the vector of local nodal displacements, $\mathbf{I}^e$ is the vector of nodal currents, $\mathbf{P}^e(\mathbf{V})$ is the vector of heat flows, and $\mathbf{F}^e(\mathbf{T})$ is the vector of local nodal forces.

In our case (2D beam element) all nodal parameters are as follows – see Fig. 2:
- unknown parameters $\mathbf{V}^e = [V_i, V_j]^T$, $\mathbf{T}^e = [T_i, T_j]^T$ and $\mathbf{u}^e = [u_i, v_i, \varphi_i, u_j, v_j, \varphi_j]^T$

- reaction parameters $\mathbf{I}^e = [I_i, I_j]^T$, $\mathbf{P}^e(\mathbf{V}) = [P_i + P_i^J, P_j + P_j^J]^T$ and

$$\mathbf{F}^e(\mathbf{T}) = [F_{xi} + F_{xi}^{th}, F_{yi}, M_i, F_{xj} + F_{xj}^{th}, F_{yj}, M_j]^T$$

All parameters (specially P_i^J, P_j^J and F_{xi}^{th}, F_{xj}^{th}) will be explained in the next sections.

3.1 FEM equations of electric conduction

After minimization of the potential energy functional (Jin 2002), we get the element matrix equation (the first line of the above-mentioned matrix Eq. (7))

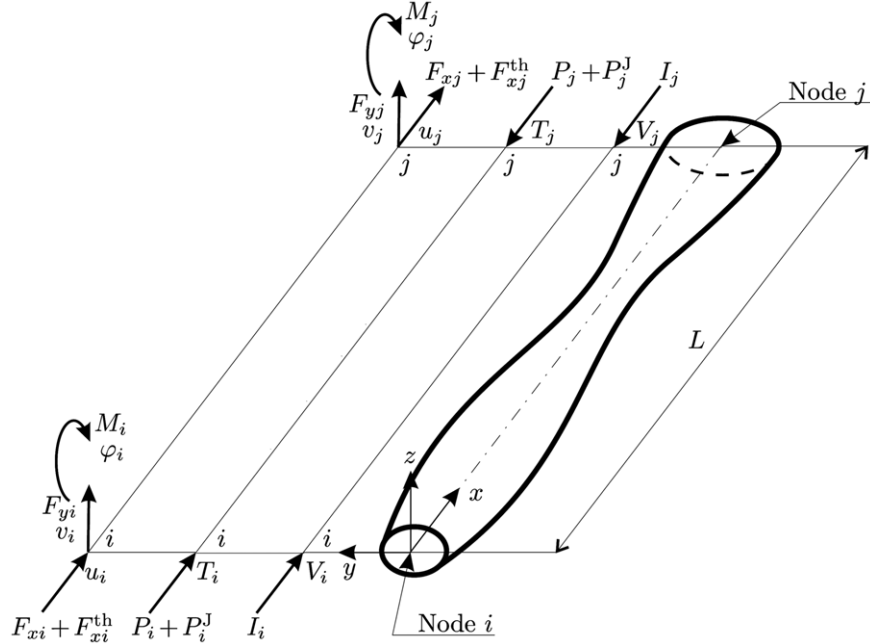$$\mathbf{K}_V^e\mathbf{V}^e = \mathbf{I}^e \tag{8}$$

Fig. 2 Coupled problem – unknown parameters and reactions

or in expanded form

$$k_V \begin{bmatrix} 1 & -1 \\ -1 & 1 \end{bmatrix} \begin{bmatrix} V_i \\ V_j \end{bmatrix} = \begin{bmatrix} I_i \\ I_j \end{bmatrix} \tag{9}$$

where $k_V = \sigma_i A_i / b'_{2A\sigma}$ is the electrical conductivity, V_i, V_j are the nodal electric potentials and I_i, I_j are the nodal currents.

Quantity $b'_{2A\sigma}$ is the transfer constant of the varying electric conductance and is defined as the first integral along the length L of expression

$$b''_{2A\sigma}(x) = \frac{1}{\eta_{A\sigma}(x)} \tag{10}$$

where the polynomial $\eta_{A\sigma}(x) = \eta_A(x)\eta_\sigma(x)$ describes the electric conductance variation. The above-mentioned transfer constant and the all following transfer constants in the below can be solved using a simple numerical algorithm (Murín and Kutiš 2002, Rubin 1999) which is briefly described in section 4.

3.2 FEM equations of heat conduction

The heat conductance relation can be expressed in a similar form to Eq. (8) as

$$\mathbf{K}_T^e \mathbf{T}^e = \mathbf{P}^e(\mathbf{V}) \tag{11}$$

or in expanded form

$$k_T \begin{bmatrix} 1 & -1 \\ -1 & 1 \end{bmatrix} \begin{bmatrix} T_i \\ T_j \end{bmatrix} = \begin{bmatrix} P_i \\ P_j \end{bmatrix} + \begin{bmatrix} P_i^J \\ P_j^J \end{bmatrix} \tag{12}$$

where $k_T = \lambda_i A_i / b'_{2A\lambda}$ is the thermal conductance, T_i, T_j are the nodal temperatures, P_i, P_j are the nodal heat flows and P_i^J, P_j^J are the Joule heat obtained by transformation of generated heat to the nodal points.

Quantity $b'_{2A\lambda}$ is the transfer constant of the varying thermal conductance and is defined as in Eq. (10), i.e., as the first integral of the following expression

$$b''_{2A\lambda}(x) = \frac{1}{\eta_{A\lambda}(x)} \tag{13}$$

where polynomial $\eta_{A\lambda}(x) = \eta_A(x)\,\eta_\lambda(x)$ describes the heat conductance variation. How to obtain the Joule heat and how to transform it into nodes is presented in the following section.

3.2.1 Computation of the Joule heat

Differential of the electrical performance is defined by the scalar product

$$dP_J(x) = \mathbf{E}(x) \cdot \mathbf{J}(x)dV = p_J(x)dV = \frac{1}{\sigma(x)}J(x)^2 dV \tag{14}$$

where $\mathbf{E}(x)$ is the electric intensity vector and $\mathbf{J}(x)$ is the current density vector. Expression $\mathbf{E}(x) \cdot \mathbf{J}(x) = p_J(x)$ is the Joule heat generated per volume. For 1D problem, the current density vector is

$$\mathbf{J}(x) = \frac{I(x)}{A(x)}\mathbf{i} = J(x)\mathbf{i} \tag{15}$$

where $\mathbf{i}$ is unit vector of x direction, $A(x)$ is the cross-sectional area where the current is applied on and $J(x)$ is the current density. The cross-sectional area and electrical conductivity along the element length have been defined by Eqs. (1) and (3), respectively. In our case, the current $I(x)$ has constant value along the element length because there is no distributed load in electric analysis, and its value is $I(x) = I = I_i = -I_j$.

The product of the cross-sectional area $A(x)$ and of the electrical performance per volume $\mathbf{E}(x) \cdot \mathbf{J}(x)$ gives the length electrical performance

$$p_{Jl}(x) = \frac{I^2}{A_i \sigma_i} \frac{1}{\eta_{A\sigma}(x)} \tag{16}$$

In thermal analysis, $p_{Jl}(x)$ represents the internal heat source distributed along the element length.

By integration of Eq. (16) along the element length L, the electrical losses (Joule heat) in element volume are given by

$$P^J(L) = P^J = \int_{(L)} p_{Jl}(x)dx = \frac{I^2}{A_i \sigma_i} \int_{(L)} \frac{1}{\eta_{A\sigma}(x)}dx \tag{17}$$

Expression (17) can be rewritten using the transfer constant $b'_{2A\sigma}$ to the form

$$P^J = \frac{I^2}{A_i \sigma_i} b'_{2A\sigma} \tag{18}$$

3.2.2 Transformation of Joule heat in the nodal heat flows vector

In thermal analysis the Joule heat per length $p_{Jl}(x)$ represents the distributed load along the element length and has to be transformed to the nodal heat flows. If we assume a functional graded materials (FGMs), the Wiedemann-Franz law does not exist between thermal and electrical conductivity because the material is mixed of metal and non-metal materials. The effective material properties are computed from the mixture rules (Altenbach *et al.* 2003). It causes unequality between electrical conductivity variation and thermal conductivity variation Eq. (22). The Wiedemann-Franz law for metal materials can be written in the form

$$k = \frac{\lambda(x)}{\sigma(x)} \tag{19}$$

where k is a constant parameter. Since k must be constant, we can write for metal materials

$$k = \frac{\lambda(x)}{\sigma(x)} = \frac{\lambda_i \eta_\lambda(x)}{\sigma_i \eta_\sigma(x)} = \frac{\lambda_i}{\sigma_i} \tag{20}$$

which suggests

$$\eta_\lambda(x) = \eta_\sigma(x) \tag{21}$$

This equation is correct for metal materials, but FGMs are a mixture of metal and non-metal materials and therefore we get

$$\eta_\lambda(x) \neq \eta_\sigma(x) \tag{22}$$

which suggests

$$k \neq \frac{\lambda(x)}{\sigma(x)} \tag{23}$$

By using a similar concept as for the transformation of distributed loads in 3D beam element (Murín and Kutiš 2002, Kutiš 2001), we can write the transformed nodal heat flow vector from the Joule heat per length $p_{Jl}(x)$. From the viewpoint of FGMs and the mixture rules, the best solution for the transformation of the Joule heat to the nodal heat flow vector is to divide the length L into halves and adequate Joule heat put to the nodal heat flow vector. It means that P_i^J represents the Joule heat generated into the first half part of the element, from 0 to $L/2$. P_j^J is the Joule heat generated into the second half part of the element, from $L/2$ to L. The nodal heat flow vector has the form

$$\begin{bmatrix} P_i^J \\ P_j^J \end{bmatrix} = \frac{I^2}{A_i \sigma_i} \begin{bmatrix} \int_0^{L/2} p_{Jl}(x) dx \\ \int_{L/2}^L p_{Jl}(x) dx \end{bmatrix} \tag{24}$$

The transformation of distributed load $p_{Jl}(x)$ according to Eq. (24) is valid for any orders of polynomials $A(x)$, $\sigma(x)$ and $\lambda(x)$.

3.3 FEM equations of structural analysis

The stiffness matrix of 2D beam element with variation of the cross-section including the 1st and 2nd order beam theory has been published in (Murín and Kutiš 2002, Kutiš 2001, Kutiš and Murín 2006). If the beam material properties are varied along the element length L, this stiffness matrix must be modified and the final equation for 2D beam with variation of cross-section and material properties has the matrix form

$$\mathbf{K}_u^e \mathbf{u}^e = \mathbf{F}^e(\mathbf{T})$$
(25)

or in expanded form

$$
\begin{bmatrix}
k_u' & 0 & 0 & -k_u' & 0 & 0 \\
 & k_{v2}' & -k_{v3}' & 0 & -k_{v2}' & -k_{v2} \\
S & & k_{v33}' & 0 & k_{v3}' & k_{v3} \\
 & Y & & k_u' & 0 & 0 \\
 & & M & & k_{v2}' & k_{v2} \\
 & & & & & k_{v23}
\end{bmatrix}
\begin{bmatrix}
u_i \\ v_i \\ \varphi_i \\ u_j \\ v_j \\ \varphi_j
\end{bmatrix}
=
\begin{bmatrix}
F_{xi} \\ F_{yi} \\ M_i \\ F_{xj} \\ F_{yj} \\ M_j
\end{bmatrix}
+
\begin{bmatrix}
F_{xi}^{\text{th}} \\ 0 \\ 0 \\ F_{xj}^{\text{th}} \\ 0 \\ 0
\end{bmatrix}
$$
(26)

where k_u' is the axial stiffness and has the form

$$k_u' = \frac{E_i A_i}{b_{2AE}'}$$
(27)

Parameters $k_{v2}, k_{v3}, k_{v2}', k_{v3}', k_{v23}$ and k_{v33}' represent the bending stiffness and their forms are

$$k_{vj} = \frac{E_i I_{yi}}{b_{2IE} b_{3IE}' - b_{3IE} b_{2IE}'} b_{jIE}, \quad \text{for} \quad j = 2, 3$$
(28)

$$k_{vj}' = \frac{E_i I_{yi}}{b_{2IE} b_{3IE}' - b_{3IE} b_{2IE}'} b_{jIE}', \quad \text{for} \quad j = 2, 3$$
(29)

$$k_{v23} = \frac{E_i I_{yi}}{b_{2IE} b_{3IE}' - b_{3IE} b_{2IE}'} (L b_{2IE} - b_{3IE})$$
(30)

$$k_{v33}' = \frac{E_i I_{yi}}{b_{2IE} b_{3IE}' - b_{3IE} b_{2IE}'} (L b_{3IE}' - b_{3IE})$$
(31)

$u_i, u_j, \ldots, \varphi_j$ are the local nodal displacements and rotations, $F_{xi}, F_{yi}, \ldots, M_j$ are the nodal forces and moments and $F_{xi}^{\text{th}}, F_{xj}^{\text{th}}$ represent the thermal loading.

The transfer constant for axial loading b_{2AE}' is defined as the first integral along the element length L of the expression

$$b_{2AE}''(x) = \frac{1}{\eta_{AE}(x)}$$
(32)

where polynomial $\eta_{AE}(x) = \eta_A(x)\eta_E(x)$ describes the axial stiffness variation. For bending transfer constants, the definition is similar as above, i.e., b_{2IE}', b_{3IE}' represent the first integral and b_{2IE}, b_{3IE} represent the second integral along the element length L of the expressions

$$b''_{2IE}(x) = \frac{1}{\eta_{IE}(x)} \qquad (33)$$

$$b''_{3IE}(x) = \frac{x}{\eta_{IE}(x)} \qquad (34)$$

where polynomial $\eta_{IE}(x) = \eta_I(x)\eta_E(x)$ describes the bending stiffness variation.

In the case of thermal loading, the thermal element nodal forces have been derived as follows

$$\begin{bmatrix} F^{th}_{xi} \\ F^{th}_{xj} \end{bmatrix} = \int_V \mathbf{B}^T\mathbf{D}\boldsymbol{\varepsilon}_0 dV = \begin{bmatrix} -1 \\ 1 \end{bmatrix} \frac{E_iA_i\alpha_{Ti}\Delta T_i}{b'_{2AE}} \int_L \eta_{\alpha\Delta T}(x)dx \qquad (35)$$

where $\mathbf{B}$ is the strain-displacement matrix, $\mathbf{D}$ is the elasticity matrix, $\boldsymbol{\varepsilon}_0$ is thermal strain matrix, $\Delta T_i = T_i - T_{ref}$ is temperature rise and T_{ref} is reference temperature. In our 1D case ($dV = A(x)dx$)

$$\mathbf{B}^T = \left[\frac{-b''_{2AE}(x)}{b'_{2AE}}, \frac{b''_{2AE}(x)}{b'_{2AE}} \right]^T \qquad (36)$$

$$\mathbf{D} = E(x) = E_i\eta_E(x) \qquad (37)$$

$$\boldsymbol{\varepsilon}_0 = \varepsilon_0(x) = \alpha_T(x)(T(x) - T_{ref}) = \alpha_{Ti}\Delta T_i\eta_\alpha(x)\eta_{\Delta T}(x) = \alpha_{Ti}\Delta T_i\eta_{\alpha\Delta T}(x) \qquad (38)$$

The polynomial of the varying temperature rise field can be derived using the shape functions of the temperature field, and has the form

$$\eta_{\Delta T}(x) = \frac{T(x) - T_{ref}}{T_i - T_{ref}} = 1 + \frac{b'_{2A\lambda}(x)}{b'_{2A\lambda}}\left(\frac{T_j - T_i}{\Delta T_i}\right) \qquad (39)$$

If the element thermal conductance is constant, then the axial variation of temperature is linear.

4. Transfer constants

Determination of the transfer functions and transfer constants occurring in the previous matrices and shape functions is based on the following expression (Rubin 1999)

$$b''_{j+2}(x) = \frac{a_j(x)}{\eta(x)} \qquad (40)$$

where the function $a_j(x) = x^j/j!$ for $j \geq 0$, and for $j \leq 0$, $a_0 = 1$, $a_j = 0$. Closed solutions for the 1st and 2nd integrals of function $b''_{j+2}(x)$ are known only for lower degree polynomials $\eta(x)$. For their numerical solution, which is more general, a recurrence rule was derived

$$b^{(n)}_j(x) = a_{j-n}(x) - \sum_{k=1}^m \eta_k\frac{(j-2+k)!}{(j-2)!}b^{(n)}_{j+k}(x), \quad \text{for} \quad j \geq 2, \; n = 0 \text{ a } 1 \qquad (41)$$

After some manipulation we get

$$b^{(n)}_j(x) = a_{j-n}(x)\sum_{t=0}^{\infty}\beta_{l,0}(x) \qquad (42)$$

where $\beta_{l,0}(x)$ is expressed by

$$\beta_{t,0}(x) = -\sum_{k=1}^{m}\left[\eta_k\beta_{t,k}(x)\prod_{r=-k}^{-1}(s-1+r)\right] \tag{43}$$

with parameters

$$s = 1 + t \qquad e = \frac{x}{s-n} \qquad \beta_{t,k} = e\beta_{t-1,k-1} \qquad \text{for} \quad k = 1,\ldots,m$$

and initial values are

$$\beta_{0,0} = 1 \qquad \beta_{0,k} = 0 \qquad \text{for} \quad k = 1,\ldots,m$$

5. Numerical experiments

5.1 Example 1 – straight actuator with variation of cross-section and material properties

A 1D-current path (actuator) with variation of the cross-section and material properties along the longitudinal axis has been considered. The aim is to perform an electro-thermo-structural analysis using the new link element. The results of this analysis will be compared with the results obtained using the classical multiphysical finite elements of code ANSYS (2007).

The current path has been chosen in a such way that constant and also varying parameters (geometry and material) have been taken into consideration. The FEM model has been created using three new link elements.

Geometry, material parameters and boundary conditions:
- geometry
  - part *I* : length $a_I = 0.1$ m, diameter $d_I = 0.02$ m
  - part *II* : length $a_{II} = 0.1$ m, diameter $d_{II}(x_{II}) = d_I (1 - 9x_{II} + 30x_{II}^2 + 100x_{II}^3)$
  - part *III* : length $a_{III} = 0.1$ m, diameter $d_{III} = 0.01$ m
- material properties
  - part *I*: electric conductivity $\sigma_I = 10000\text{Sm}^{-1}$, thermal conductivity $\lambda_I = 40$ W/mK, elasticity modulus $E_I = 2 \times 10^{11}$ Pa, thermal expansion coefficient $\alpha_{TI} = 1 \times 10^{-5}\text{K}^{-1}$
  - part *II*: electric conductivity $\sigma_{II} = \sigma_I (1 + 20x_{II}^2 + 200x_{II}^3)$, thermal conductivity $\lambda_{II} = \lambda_I (1 + x_{II}^2 + 200x_{II}^3)$, elasticity modulus $E_{II} = E_I (1 + 50x_{II}^2 + 500x_{II}^3)$, thermal expansion coefficient $\alpha_{TII} = \alpha_{TI} (1 + 200x_{II}^2 + 2000x_{II}^3)$
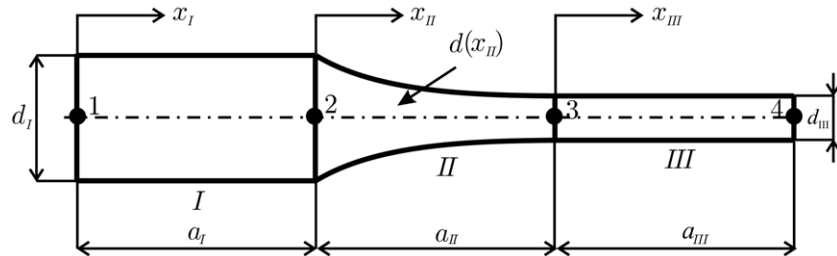

Fig. 3 1D-current path (actuator)

– part *III*: electric conductivity $\sigma_{III} = 14000 \mathrm{Sm}^{-1}$, thermal conductivity $\lambda_{III} = 56$ W/mK, elasticity modulus $E_{III} = 4 \times 10^{11}$ Pa, thermal expansion coefficient $\alpha_{TIII} = 5 \times 10^{-5} \mathrm{K}^{-1}$

– reference temperature: $T_{\mathrm{ref}} = 273$K

• boundary conditions

  – electrical: current $I_4 = 1$A, potential $V_1 = 20$V

  – thermal: thermal flow $P_1 = 1$W, temperature $T_4 = 323$K

  – structural: in the static determined case (SD): $u_1 = 0$ m, in static undetermined case (SU): $u_1 = u_4 = 0$ m

The global FEM equation for electric analysis has the form

$$\begin{bmatrix} k_V^I & -k_V^I & 0 & 0 \\ -k_V^I & k_V^I + k_V^{II} & -k_V^{II} & 0 \\ 0 & -k_V^{II} & k_V^{II} + k_V^{III} & -k_V^{III} \\ 0 & 0 & -k_V^{III} & k_V^{III} \end{bmatrix} \begin{bmatrix} V_1 \\ V_2 \\ V_3 \\ V_4 \end{bmatrix} = \begin{bmatrix} I_1 \\ 0 \\ 0 \\ I_4 \end{bmatrix} \tag{44}$$

The global electric conductance matrix contains the conductance k_V^e of elements 1, 2 and 3. After applying electric boundary conditions, the following values of unknowns have been determined: $V_2 = 20.0318$ V, $V_3 = 20.1016$ V, $V_4 = 20.1925$ V and current $I_1 = 1$ A. The Joule heat in a volume element can be solved using expression (17) and its transformation into element nodes can be performed by (24). Their values in individual nodes are: $P_1^{J,1} = P_2^{J,1} = 0.0159155$ W, $P_2^{J,2} = P_3^{J,2} = 0.0454728$ W, $P_3^{J,3} = P_4^{J,3} = 0.0454728$ W, where the second superscript represents the element number. Joule heat per length and current density are shown in Fig. 4.

The heat conductance equations of the current path have the form

$$\begin{bmatrix} k_T^I & -k_T^I & 0 & 0 \\ -k_T^I & k_T^I + k_T^{II} & -k_T^{II} & 0 \\ 0 & -k_T^{II} & k_T^{II} + k_T^{III} & -k_T^{III} \\ 0 & 0 & -k_T^{III} & k_T^{III} \end{bmatrix} \begin{bmatrix} T_1 \\ T_2 \\ T_3 \\ T_4 \end{bmatrix} = \begin{bmatrix} P_1 \\ 0 \\ 0 \\ P_4 \end{bmatrix} + \begin{bmatrix} P_1^{J,I} \\ P_2^{J,I} + P_2^{J,II} \\ P_3^{J,II} + P_3^{J,III} \\ P_4^{J,III} \end{bmatrix} \tag{45}$$
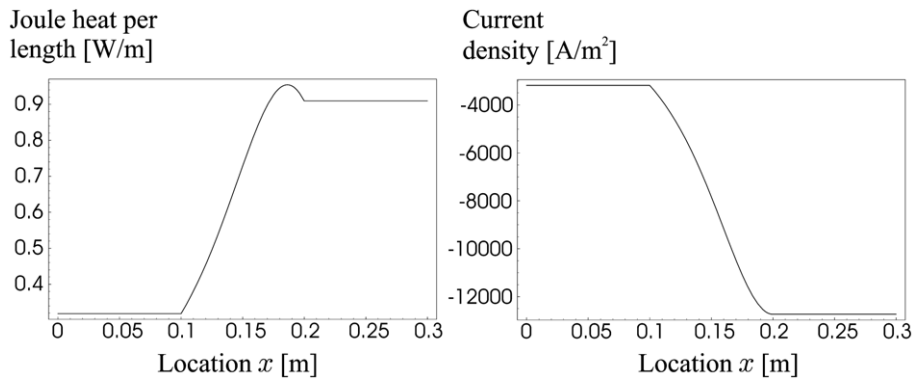

Fig. 4 Example 1 – Joule heat per length and current density
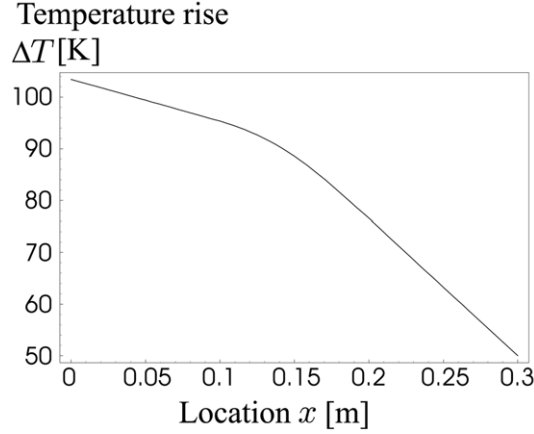
Temperature rise
ΔT [K]

Fig. 5 Example 1 – the distribution of temperature rise along the actuator length

where the thermal conductance matrix contains the element conductance k_T^e of elements. After applying thermal boundary conditions the nodal temperatures have been solved: $T_1 = 375.8$ K, $T_2 = 367.7$ K, $T_3 = 349.1$ K. The distribution of temperature rise along the current path is shown in Fig. 5.

In order to obtain deformation of the system, the determined nodal temperatures from thermal analysis have to be used as thermal loads in the structural analysis. Thermal loads are transfered to the structural loads through the thermal element nodal force-expression (35). For a statically undetermined case (SU) the stiffness relation has the form

$$\begin{bmatrix} k_u^I & -k_u^I & 0 & 0 \\ -k_u^I & k_u^I + k_u^{II} & -k_u^{II} & 0 \\ 0 & -k_u^{II} & k_u^{II} + k_u^{III} & -k_u^{III} \\ 0 & 0 & -k_u^{III} & k_u^{III} \end{bmatrix} \begin{bmatrix} u_1 \\ u_2 \\ u_3 \\ u_4 \end{bmatrix} = \begin{bmatrix} R_1 \\ 0 \\ 0 \\ R_4 \end{bmatrix} + \begin{bmatrix} -F_1^{\mathrm{th},I} \\ F_2^{\mathrm{th},I} - F_2^{\mathrm{th},II} \\ F_3^{\mathrm{th},II} - F_3^{\mathrm{th},III} \\ F_4^{\mathrm{th},III} \end{bmatrix} \qquad (46)$$

where R_1 and R_4 are reactions in the constraints, and $F_1^{\mathrm{th},e}$ to $F_4^{\mathrm{th},e}$ are the nodal thermal forces according to expression (35). Their values are: $F_1^{\mathrm{th},I} = F_2^{\mathrm{th},I} = 62027.29$ N, $F_2^{\mathrm{th},II} = F_3^{\mathrm{th},II} = 59878.37$ N, $F_3^{\mathrm{th},III} = F_4^{\mathrm{th},III} = 99022.21$ N. In the statically determined case (SD), the reactions are equal to zero, and on the right hand side of Eq. (46) we get only thermal forces.

For a statically undetermined case (SU) we get: $u_2 = -2.345 \times 10^{-5}$ m, $u_3 = -7.085 \times 10^{-5}$ m, and $R_1 = -R_4 = 76763.4$ N, and for the statically determined case (SD): $u_2 = 0.9872 \times 10^{-4}$ m, $u_3 = 2.810 \times 10^{-4}$ m, $u_4 = 5.960 \times 10^{-4}$ m.

The same problem has been solved using the multiphysical element LINK68 (ANSYS 2007). To show the effectiveness and accuracy of our element each of the three parts of the current path was divided to 1, 10, and 150 LINK68 elements. The comparison of the two solution results is given in Tables 1, 2 and 3. The last line in these tables contains the results obtained using only one our link element for each part of the conductor. The comparison of results shows that the LINK68 results converge anyway to our element results.

Table 1 Comparison of the nodal variables – potential and temperature rise

NOE	Electric potential [V]			Temperature rise [K]		
	V_2	V_3	V_4	ΔT_1	ΔT_2	ΔT_3
1	20.031	20.104	20.195	103.693	95.600	76.151
10	20.031	20.101	20.192	102.777	94.682	76.081
150	20.032	20.102	20.193	102.760	94.677	76.080
1	20.032	20.101	20.192	102.762	94.677	76.079

Table 2 Comparison of the nodal variables – displacement, SU and SD case

NOE	Displacements – SU $\times 10^{-5}$ [m]		Displacement – SD $\times 10^{-4}$ [m]		
	u_2	u_3	u_2	u_3	u_4
1	−1.180	−9.246	0.965	2.499	5.653
10	−2.354	−7.146	0.987	2.808	5.969
150	−2.365	−7.127	0.987	2.811	5.972
1	−2.345	−7.085	0.9872	2.810	5.960

Table 3 Reactions and stress in SU case

NOE	Reactions [N]	Stress [MPa]	
	$R_1 = -R_2$	σ_1	σ_3
1	70030	−222.9	−891.6
10	76842	−244.6	−978.3
150	76907	−244.8	−979.2
1	76763.4	−243.3	−977.4

From these tables it can be seen that the maximal difference between both analyses occurs in the results of structural variables.

5.2 Example 2 – Electro-thermo-structural analysis of the FGM actuator

Electro-thermo-mechanical actuator with variation of a rectangular cross-section and material properties has been considered (Fig. 6). The actuator is made from functional graded materials (FGMs). The actuator is loaded by an electric current and has an ideal thermal insulation. The goal is to perform an electro-thermo-structural analysis using the new beam element. The results of this analysis will be compared with the results obtained using the coupled analysis with classical electro-thermal link and structural beam elements of code ANSYS (2007).

The FEM-model has been created with only six new beam elements.

Geometry, material properties and boundary conditions:

• geometry

Whole actuator has the same width $w = 0.003$ m.

– part *I*: length $a_I = 0.02$ m, hight $h_I(x_I) = 2(0.003 - 0.15x + 3.75x^2)$m

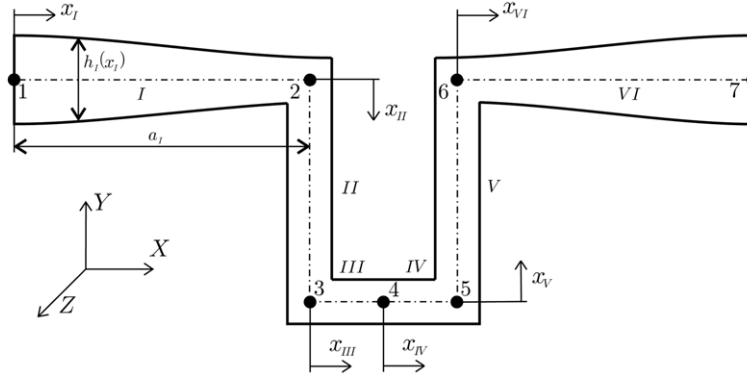– part *II*: length $a_{II} = 0.015$ m, hight $h_{II} = 0.003$ m

Fig. 6 Electro-thermo-mechanical actuator from FGMs materials

− part *III*: length a_{III} = 0.005 m, hight h_{III} = 0.003 m
− part *IV*: length a_{IV} = 0.005 m, hight h_{IV} = 0.003 m
− part *V*: length a_V = 0.015 m, hight h_V = 0.003 m
− part *VI*: length a_{VI} = 0.02 m, hight $h_{VI}(x_I)$ = 2(0.0015 + 3.75x^2)m

• material properties

Each part of the actuator is made from FGM. The parts consist of two different materials, namely matrix and fibre. The rule of mixture for the volume fraction of each material (Altenbach *et al.* 2003) has been used to determine effective constitutive properties (CP) of each part. FGM has a unidirectional variation of the fibres along the axis of the part and therefore the effective CP will also be varied along the part length according to expression

$$X(x) = X_f v_f(x) + X_m v_m(x) = X_f v_f(x) + X_m(1 - v_f) \tag{47}$$

because

$$V = V_f + V_m, \ \frac{V_f}{V} + \frac{V_m}{V} = v = v_f + v_m = 1 \tag{48}$$

where, $X(x)$ is the effective constitutive property, X_f and X_m are CPs of the fiber and matrix, respectively, $v_f(x)$ and $v_m(x)$ are volume fractions of the fiber and of matrix, respectively.

Individual parts have the following fiber, matrix and effective material properties:
− part *I*: fiber Al_2O_3, matrix *Fe*,
v_f = 0.05 + 375x_I^2 − 12500x_I^3,
electric conductivity
σ_{If} = 1 × 10^{-12} Sm^{-1}, σ_{Im} = (7.6 × 10^{-7})$^{-1}$ Sm^{-1},
σ_I = 65789.5(1 + 7500x_I^2 − 250000x_I^3)Sm^{-1},
thermal conductivity
λ_{If} = 25 W/mK, λ_{Im} = 60.5 W/mK,
λ_I = 26.775(1 + 497.199x_I^2 − 16573.296x_I^3)W/mK,
elasticity modulus
E_{If} = 300 GPa, E_{Im} = 200 GPa,

$E_I = 295(1 - 127.1186 x_I^2 + 4237.2881 x_I^3)$GPa,

thermal expansion coefficient

$\alpha_{If} = 7.5 \times 10^{-6}\,\mathrm{K}^{-1}$, $\alpha_{Im} = 15.3 \times 10^{-6}\,\mathrm{K}^{-1}$,

$\alpha_{TI} = (7.1289 \times 10^{-6})(1 - 390.4203 x_I^2 + 13014 x_I^3)\mathrm{K}^{-1}$

– part *II*: fiber Al_2O_3, matrix *Fe*,

$v_f = 0.1 - 666.667 x_{II}^2 + 29629.63 x_{II}^3$,

electric conductivity

$\sigma_{IIf} = 1 \times 10^{-12}\,\mathrm{Sm}^{-1}$, $\sigma_{IIm} = (7.6 \times 10^{-7})^{-1}\,\mathrm{Sm}^{-1}$,

$\sigma_{II} = 131579(1 - 6666.667 x_{II}^2 + 296296.296 x_{II}^3)\mathrm{Sm}^{-1}$,

thermal conductivity

$\lambda_{IIf} = 25$ W/mK, $\lambda_{IIm} = 60.5$ W/mK,

$\lambda_{II} = 28.55(1 - 828.955 x_{II}^2 + 36842.447 x_{II}^3)$W/mK,

elasticity modulus

$E_{IIf} = 300$ GPa, $E_{IIm} = 200$ GPa,

$E_{II} = 290(1 + 229.885 x_{II}^2 - 10217.113 x_{II}^3)$GPa,

thermal expansion coefficient

$\alpha_{IIf} = 7.5 \times 10^{-6}\,\mathrm{K}^{-1}$, $\alpha_{IIm} = 15.3 \times 10^{-6}\,\mathrm{K}^{-1}$,

$\alpha_{TII} = (6.7578 \times 10^{-6})(1 + 732.196 x_{II}^2 - 32542.032 x_{II}^3)\mathrm{K}^{-1}$

– part *III*: fiber *Fe*, matrix *Cu*,

$v_f = 0.1 - 6000 x_{III}^2 + 800000 x_{III}^3$,

electric conductivity

$\sigma_{IIIf} = (7.6 \times 10^{-7})^{-1}\,\mathrm{Sm}^{-1}$, $\sigma_{IIIm} = (1.71 \times 10^{-8})^{-1}\,\mathrm{Sm}^{-1}$,

$\sigma_{III} = 7032163.743(1 - 48773.389 x_{III}^2 + 6503118.503 x_{III}^3)\mathrm{Sm}^{-1}$,

thermal conductivity

$\lambda_{IIIf} = 60.5$ W/mK, $\lambda_{IIIm} = 391$ W/mK,

$\lambda_{III} = 93.55(1 - 21197.221 x_{III}^2 + 2.826 \times 10^6 x_{III}^3)$W/mK,

elasticity modulus

$E_{IIIf} = 200$ GPa, $E_{Im} = 115$ GPa,

$E_{III} = 191.5(1 + 2663.185 x_{III}^2 - 355091.384 x_{III}^3)$GPa,

thermal expansion coefficient

$\alpha_{IIIf} = 15.3 \times 10^{-6}\,\mathrm{K}^{-1}$, $\alpha_{IIIm} = 17 \times 10^{-6}\,\mathrm{K}^{-1}$,

$\alpha_{TIII} = (1.770 \times 10^{-6})(1 - 57357.652 x_{III}^2 + 764768.697 x_{III}^3)\mathrm{K}^{-1}$

– part *IV*: fiber *Fe*, matrix *Cu*,

$v_f = 0.05 + 6000 x_{IV}^2 - 800000 x_{IV}^3$,

electric conductivity

$\sigma_{IVf} = (7.6 \times 10^{-7})^{-1}\,\mathrm{Sm}^{-1}$, $\sigma_{IVm} = (1.71 \times 10^{-8})^{-1}\,\mathrm{Sm}^{-1}$,

$\sigma_{IV} = 7032163.743(1 + 82171.629 x_{IV}^2 - 10956217.163 x_{IV}^3)\mathrm{Sm}^{-1}$,

thermal conductivity

$\lambda_{IVf} = 60.5$ W/mK, $\lambda_{IVm} = 391$ W/mK,

$\lambda_{IV} = 77.025(1 + 25744.888 x_{IV}^2 - 3432651.736 x_{IV}^3)$W/mK,

elasticity modulus

$E_{IVf} = 200$ GPa, $E_{Im} = 115$ GPa,

$E_{IV} = 195.75(1 - 2605.364 x_{IV}^2 + 347381.865 x_{IV}^3)$GPa,

thermal expansion coefficient

$\alpha_{IVf} = 15.3 \times 10^{-6}\,\mathrm{K}^{-1}$, $\alpha_{IVm} = 17 \times 10^{-6}\,\mathrm{K}^{-1}$,

$$\alpha_{TIV} = 9.241 \times 10^{-7}(1 + 109876.442x_{IV}^2 - 14650192.233x_{IV}^3)\text{K}^{-1}$$

– part *V*: fiber Al_2O_3, matrix *Fe*,

$$v_f = 0.05 + 666.667x_V^2 - 29629.63x_V^3,$$

electric conductivity

$$\sigma_{Vf} = 1 \times 10^{-12}\,\text{Sm}^{-1}, \ \sigma_{Vm} = (7.6 \times 10^{-7})^{-1}\,\text{Sm}^{-1},$$

$$\sigma_V = 65789.5(1 + 13333.333x_V^2 - 592592.593x_V^3)\text{Sm}^{-1},$$

thermal conductivity

$$\lambda_{Vf} = 25 \ \text{W/mK}, \ \lambda_{Vm} = 60.5 \ \text{W/mK}$$

$$\lambda_V = 28.55(1 - 828.955x_V^2 + 36842.447x_V^3)\text{W/mK},$$

$$\lambda_V = 26.775(1 + 883.91x_V^2 - 39284.85x_V^3)\text{W/mK},$$

elasticity modulus

$$E_{Vf} = 300 \ \text{GPa}, \ E_{Im} = 200 \ \text{GPa},$$

$$E_V = 295(1 - 225.989x_V^2 + 10043.942x_V^3)\text{GPa},$$

thermal expansion coefficient

$$\alpha_{Vf} = 7.5 \times 10^{-6}\,\text{K}^{-1}, \ \alpha_{Vm} = 15.3 \times 10^{-6}\,\text{K}^{-1},$$

$$\alpha_{TV} = (7.1289 \times 10^{-6}(1 - 694.0805x_V^2 + 30848.023x_V^3)\text{K}^{-1}$$

– part *VI*: fiber Al_2O_3, matrix *Fe*,

$$v_f = 0.1 - 375x_{VI}^2 + 12500x_{VI}^3,$$

electric conductivity

$$\sigma_{VIf} = 1 \times 10^{-12}\,\text{Sm}^{-1}, \ \sigma_{VIm} = (7.6 \times 10^{-7})^{-1}\,\text{Sm}^{-1},$$

$$\sigma_{VI} = 131579(1 - 3750x_{VI}^2 + 125000x_{VI}^3)\text{Sm}^{-1},$$

thermal conductivity

$$\lambda_{VIf} = 25 \ \text{W/mK}, \ \lambda_{VIm} = 60.5 \ \text{W/mK},$$

$$\lambda_{VI} = 28.55(1 - 466.287x_{VI}^2 + 15542.907x_{VI}^3)\text{W/mK},$$

elasticity modulus

$$E_{VIf} = 300 \ \text{GPa}, \ E_{VIm} = 200 \ \text{GPa},$$

$$E_{VI} = 290(1 + 129.310x_{VI}^2 - 4310.3448x_{VI}^3)\text{GPa},$$

thermal expansion coefficient

$$\alpha_{VIf} = 7.5 \times 10^{-6}\,\text{K}^{-1}, \ \alpha_{VIm} = 15.3 \times 10^{-6}\,\text{K}^{-1},$$

$$\alpha_{TVI} = 6.7578 \times 10^{-6}(1 + 411.860x_{VI}^2 - 13728.67x_{VI}^3)\text{K}^{-1}$$

– reference temperature: $T_{\text{ref}} = 273\text{K}$

• boundary conditions
  – electrical: current $I_7 = 2\text{A}$, potential $V_1 = 20\text{V}$
  – thermal: thermal flow $P_1 = 0\text{W}$, temperature $T_7 = T_{\text{ref}} = 273\text{K}$
  – structural: in static undetermined case(SU): $u_{x1} = u_{y1} = 0$ m, $\varphi_{z1} = 0°$, $u_{x7} = u_{y7} = 0$ m, $\varphi_{z7} = 0°$

This coupled problem has been solved as sequential coupling. In the first step the electric analysis has been performed according to Eq. (9). The output from this analysis has been the transformed Joule heat – Eq. (24). The second analysis has been thermal analysis – Eq. (12), where the determined Joule heat has been used as loading. The output from this analysis have been thermal forces which are computed according to Eq. (35). The last step has been to perform structural analysis – Eq. (26), where the determined thermal forces act as loads. The final output was structural displacements and rotations and also reaction forces and moments. The deformed and undeformed shape is shown in Fig. 7.
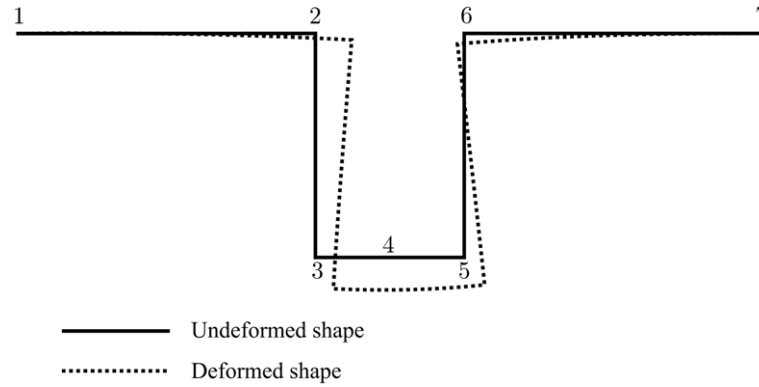
Fig. 7 Example 2 – deformed and undeformed shape of actuator

The same problem has been analyzed by a sequential method using the multiphysical element LINK68 and beam element BEAM3 (ANSYS 2007). To show the effectiveness and accuracy of our element each of the six parts of the actuator was divided to 1 and 25 elements. LINK68 element is used for the electro-thermal analysis and BEAM3 element is used for the structural analysis. The comparison of the two solution results is given in Tables 4-10. The last line in these tables contains the results obtained using only one our link/beam element for each part of the actuator.

Table 4 Comparison of the nodal variables - Electric potential [V]

NOE	Electric potential [V]					
	V_1	V_2	V_3	V_4	V_5	V_6
1	20.0360	20.0698	20.0700	20.0702	20.1040	20.1400
25	20.0356	20.0714	20.0716	20.0718	20.1075	20.1431
1	20.0356	20.0714	20.0716	20.0718	20.1075	20.1433

Table 5 Comparison of the nodal variables - Temperature rise [K]

NOE	Temperature rise [K]					
	ΔT_1	ΔT_2	ΔT_3	ΔT_4	ΔT_5	ΔT_6
1	36.6916	34.3761	27.9994	27.0886	26.1753	15.6806
25	37.1214	34.6131	28.4347	27.4994	26.5612	15.4821
1	37.1195	34.8210	28.8313	27.8961	26.9579	15.6906

Table 6 Comparison of the nodal variables - Displacements U_x [m]

NOE	Displacements U_{xi} [$\times 10^{-6}$m]				
	U_{x2}	U_{x3}	U_{x4}	U_{x5}	U_{x6}
1	4.9047	2.24937	2.42084	2.58616	−1.05899
25	5.02142	2.46304	2.63814	2.8059	−0.97073
1	4.98519	2.46033	2.63824	2.80881	−0.93455

Table 7 Comparison of the nodal variables - Displacements U_y [m]

NOE	Displacements U_{yi} [$\times 10^{-6}$ m]				
	U_{y2}	U_{y3}	U_{y4}	U_{y5}	U_{y6}
1	−1.4252	−4.6715	−4.8434	−4.2550	−2.0734
25	−0.94808	−4.2661	−4.3807	−3.7385	−1.5108
1	−0.9347	−4.24733	−4.35789	−3.71962	−1.49722

Table 8 Comparison of the nodal variables - Rotation Rot_z [rad]

NOE	Rotation Rot_{zi} [$\times 10^{-6}$ rad]				
	Rot_{z2}	Rot_{z3}	Rot_{z4}	Rot_{z5}	Rot_{z6}
1	−148.41	−112.59	42.729	191.53	201.45
25	−147.63	−102.35	54.287	201.71	210.58
1	−145.735	−100.732	54.3004	200.119	208.689

Table 9 Comparison of the reactions

NOE	Electric-Thermal reactions	
	I_1 [A]	P_7 [W]
1	−2	−0.28002
25	−2	−0.28629
1	−2	−0.28628

Table 10 Comparison of the reactions

NOE	Structural reactions					
	F_{x1} [N]	F_{y1} [N]	M_{z1} [Nm]	F_{x7} [N]	F_{y7} [N]	M_{z7} [Nm]
1	4.8985	−0.34088	0.02521	−4.8985	0.34088	−0.04225
25	4.8066	−0.47934	0.02038	−4.8066	0.47934	−0.044346
1	4.75607	−0.479534	0.020035	−4.75607	−0.479534	−0.044011

The comparison of result shows very good effectiveness of the new link/beam finite element.

6. Conclusions

A new multiphysical two nodal link finite element has been presented in this contribution which can be used for effective solving of weak coupled electro-thermo-structural problems. Polynomial variations of electric and thermal conductance, thermal expansion coefficient and elasticity modulus have been taken into consideration. The element matrix and the right hand side vector containing the Joule heat and thermal forces have been derived. The 1D electric and temperature field can be coupled from the stiffness element matrix point of view with the bar or with the beam finite element (with varying stiffness and thermal expansion coefficient) as well. The basic element

relations contain transfer constants which depend on variations of geometry and material properties. These transfer constants can be solved using the simple numerical algorithm. The results of numerical experiment prove the effectiveness and accuracy of our new element for a coarse mesh - the solution accuracy does not depend on the mesh density. Using a finer mesh has no effect on the obtained results. This new element can be very effectively used for electro-thermo-structural analysis of constructional parts built from composite or uni-axially graded materials.

Acknowledgements

References

Agarwal, S., Chakraborty, A. and Gopalakrishnaw, S. (2006), "Large deformation analysis for anisotropic inhomogeneous beams using exact linear static solution", *Compos. Struct.*, **72**(1), 91-104.

Altenbach, H., Altenbach, J. and Kissing, W. (2003), *Mechanics of Composite Structural Elements*, Engineerig-Monograph (English), Springer-Verlag.

ANSYS 10.0 (2007), Theory Manual.

Atluri, S.N. and Shen, S. (2004), *The Meshless Local Petrov-Galerkin Method*, Tech Science Press.

Chakraborty, A., Gopalakrishnan, S. and Reddy, J.N. (2003), "A new beam finite element forthe analysis of functionally graded materials", *Int. J. Mech. Sci.*, **45**, 519-539.

Felippa, C.A. and Park, K.C. (2004), Synthesis Tools for Structural Dynamics and Partitioned Analysis of Coupled Systems, NATO-ARW Workshop on Multi-physics and Multiscale Computer Models in Non-linear Analysis and Optimal Design of Engineering Structures Under Extreme Conditions, Bled, Slovenia, 13-17 June.

FGM Forum (1991), Survey for Application of FGM, The Society of Non-Traditional Technology, Tokyo.

http://www.eumat.org, European Technology Platform on Advanced Engineering Materials and Technologies, 2006.

Jin, J. (2002), *The Finite Element Method in Electromagnetics*, John Wiley and Sons.

Kawasaki, A. and Watanabe, R. (1997), "Concept and P/M fabrication of functionallygradient materials", *Ceramics Int.*, **23**(1), 73-83.

Koizumi, M. (1997), *FGM Activity in Japan*, Composites, No. 28B, Volume Part B.

Koizumi, M. and Niino, M. (1995), *Overview of FGM Research in Japan*, MRS Bulletin, No. 20, pp.19-21.

Kutiš, V. and Murín, J. (2006), "Stability of a slender beam-column with locally varying Young's modulus", *Struct. Eng. Mech., An Int. J.*, **23**(1), 15-27.

Kutiš, V. (2001), "Beam element with variation of cross-section satisfying local and global equilibrium conditions", Ph.D. thesis, Slovak University of Technology, Bratislava.

Lee, J.L. (2005), "Layerwise laminate analysis of functionally graded piezoelectric bimorph beams", *J. Intelligent Mater. Syst. Struct.*, **16**(4), 365-371.

Murín, J. and Kutiš, V. (2002), "3D-beam element with continuous variation of the cross-sectional area", *Comput. Struct.*, **80**, 329-338.

Müller, E., Drašar, Č., Schilz, J. and Kaysser, W.A. (2003), "Functionally graded materials for sensor and energy applications", *Mater. Sci. Eng. A*, **362**(1-2), 17-39.

Rubin, H. (1999), Bautechnik, Köln, Ernst and Sohn.

Zhu, H. and Sankar, B.H. (2004), "A Combine Fourier series-Galerkin method for the analysis of functionally graded beams", *J. Appl. Mech.*, **71**(3), 421-424.